Mineralogical Magazine, October 2017, Vol. 81(5), pp. 1141–1149

Currierite, $Na_4Ca_3MgAl_4(AsO_3OH)_{12}\cdot 9H_2O$, a new acid arsenate with ferrinatrite-like heteropolyhedral chains from the Torrecillas mine, Iquique Province, Chile

Anthony R. Kampf[1,*], Stuart J. Mills[2], Barbara P. Nash[3], Maurizio Dini[4] and Arturo A. Molina Donoso[5]

[1] Mineral Sciences Department, Natural History Museum of Los Angeles County, 900 Exposition Boulevard, Los Angeles, CA 90007, USA
[2] Geosciences, Museum Victoria, GPO Box 666, Melbourne 3001, Australia
[3] Department of Geology and Geophysics, University of Utah, Salt Lake City, Utah 84112, USA
[4] Pasaje San Agustin 4045, La Serena, Chile
[5] Los Algarrobos 2986, Iquique, Chile

[*Received 29 August 2016; Accepted 9 November 2016; Associate Editor: Andrew Christy*]

ABSTRACT

The new mineral currierite (IMA2016-030), $Na_4Ca_3MgAl_4(AsO_3OH)_{12}\cdot 9H_2O$, was found at the Torrecillas mine, Iquique Province, Chile, where it occurs as a secondary alteration phase in association with anhydrite, canutite, chudobaite, halite, lavendulan, magnesiokoritnigite, quartz, scorodite and torrecillasite. Currierite occurs as hexagonal prisms, needles and hair-like fibres up to ~200 μm long, in sprays. The crystal forms are {100} and {001}. Crystals are transparent, with vitreous to silky lustre and white streak. The Mohs hardness is ~2, tenacity is brittle, but elastic in very thin fibres, and the fracture is irregular. Crystals exhibit at least one good cleavage parallel [001]. The measured density is 3.08(2) g cm^{-3} and the calculated density is 3.005 g cm^{-3}. Optically, currierite is uniaxial (–) with $\omega = 1.614(1)$ and $\varepsilon = 1.613(1)$ (measured in white light). The mineral is slowly soluble in dilute HCl at room temperature. The empirical formula, determined from electron-microprobe analyses, is $(Na_{3.95}Al_{2.96}Ca_{2.74}Mg_{1.28}Fe^{3+}_{0.63}Cu_{0.13}K_{0.08}Co_{0.03})_{\Sigma 11.80}(As^{5+}_{11.68}Sb^{5+}_{0.32})_{\Sigma 12}(O_{56.96}Cl_{0.04})_{\Sigma 57}H_{30.81}$. Currierite is hexagonal, $P622$, with $a = 12.2057(9)$, $c = 9.2052(7)$ Å, $V = 1187.7(2)$ Å^3 and $Z = 1$. The eight strongest powder X-ray diffraction lines are [d_{obs} Å(I)(hkl)]: 10.63(100)(100), 6.12(20)(110), 5.30(15)(200), 4.61(24)(002), 4.002(35)(210), 3.474(29)(202), 3.021(96)(212) and 1.5227(29)(440,334,612). The structure of currierite ($R_1 = 2.27\%$ for 658 $F_o > 4\sigma F$ reflections) is based upon a heteropolyhedral chain along **c** in which AlO_6 octahedra are triple-linked by sharing corners with AsO_3OH tetrahedra. Chains are linked to one another by bonds to 8(4 + 4)-coordinated Na and 8-coordinated Ca forming a three-dimensional framework with large cavities that contain rotationally disordered $Mg(H_2O)_6$ octahedra. The chain in the structure of currierite is identical to that in kaatialaite and a geometrical isomer of that in ferrinatrite. The mineral is named in honour of Mr. Rock Henry Currier (1940–2015), American mineral dealer, collector, author and lecturer.

Keywords: currierite, new mineral, acid arsenate, crystal structure, kaatialaite, ferrinatrite, Torrecillas mine, Chile.

Introduction

The Torrecillas mine, in the northern Atacama Desert of Chile, is a small, long-inactive arsenic mine. Over the last several years, investigations of the minerals of this unusual deposit have yielded many new and potentially new mineral species. To

*E-mail: akampf@nhm.org
https://doi.org/10.1180/minmag.2016.080.167

FIG. 1. Sprays of currierite fibres with anhydrite, lavendulan and halite on scorodite. Field of view 3 mm across.

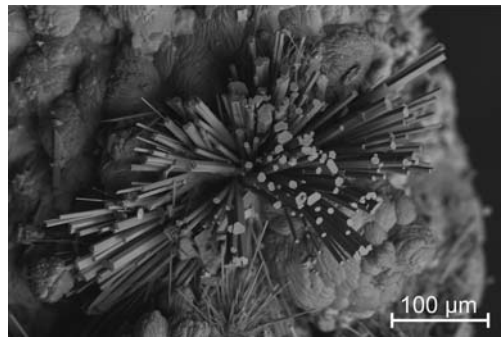

FIG. 2. Back-scatter electron image of currierite needles on scorodite.

date, the descriptions of seven new minerals have been published: leverettite (Kampf *et al.*, 2013*a*), magnesiokoritnigite (Kampf *et al.*, 2013*b*), torrecillasite (Kampf *et al.*, 2014*b*), canutite (Kampf *et al.*, 2014*a*), chongite (Kampf *et al.*, 2016*a*), gajardoite (Kampf *et al.*, 2016*b*) and juansilvaite (Kampf *et al.*, 2016*c*). Herein, we describe the eighth new mineral from the Torrecillas mine, currierite. Several other potentially new minerals are still under study.

The mineral is named in honour of Mr. Rock Henry Currier (1940–2015), American mineral dealer, collector, author and lecturer. Rock was the owner/operator of a successful wholesale mineral and lapidary import and supply business, Jewel Tunnel Imports, in the Los Angeles, California area. He loved travelling to out-of-the-way locales in search of specimen material (including Peru, Bolivia and northern Chile) and he loved sharing his experiences. His legendary sense of humour, often straying into the risqué, but never mean-spirited, was one of his many endearing qualities. Another was his unrelenting effort to benefit the greater mineralogical community. He did this locally through his longstanding leadership role in the Mineralogical Society of Southern California, and on the national and international stages by delighting audiences with his wonderful programs and articles (e.g. Currier 1995, 2008*a*,*b*, 2009*a*,*b*,*c*). He was always generous in providing

TABLE 1. Analytical data (wt.%) for currierite.

Constituent	Mean	Range	S.D.	Standard
K_2O	0.17	0.14–0.20	0.04	sanidine
Na_2O	5.65	5.16–6.39	0.46	albite
CaO	7.10	6.76–7.54	0.28	diopside
MgO	2.39	2.35–2.44	0.04	diopside
CoO	0.09	0.04–0.16	0.05	Co metal
CuO	0.47	0.36–0.58	0.10	Cu metal
Fe_2O_3	2.32	2.13–2.74	0.24	hematite
Al_2O_3	6.97	6.70–7.57	0.43	syn. YAG
Sb_2O_5	2.42	1.96–3.01	0.42	syn. GaSb
As_2O_5	62.03	59.69–64.19	1.80	syn. GaAs
Cl	0.07	0.05–0.12	0.03	tugtupite
H_2O*	12.82			
O=Cl	–0.02			
Total	102.48			

* Calculated on the basis of As + Sb = 12 apfu, charge balance and O + Cl = 57 apfu. S.D. – standard deviation.

TABLE 2. Powder X-ray data for currierite.

I_{obs}	d_{obs}	d_{calc}	I_{calc}	$h\ k\ l$	I_{obs}	d_{obs}	d_{calc}	I_{calc}	$h\ k\ l$
100	10.63	10.5705	100	1 0 0			1.8438	1	4 1 3
3	9.19	9.2052	3	0 0 1	7	1.8338	1.8374	2	2 2 4
20	6.12	6.1029	18	1 1 0			1.8325	2	4 2 2
15	5.30	5.2852	11	2 0 0	13	1.8106	1.8102	9	3 1 4
24	4.61	4.6026	14	0 0 2	15	1.7374	1.7378	3	4 3 0
		4.5835	2	2 0 1			1.7355	8	4 0 4
4	4.230	4.2199	3	1 0 2	3	1.6917	1.6926	2	5 2 0
35	4.002	3.9953	29	2 1 0			1.6741	1	4 2 3
9	3.679	3.6747	3	1 1 2	4	1.6689	1.6693	1	3 2 4
		3.6649	4	2 1 1			1.6647	1	5 2 1
7	3.527	3.5235	3	3 0 0	10	1.6444	1.6453	7	6 0 2
29	3.474	3.4710	22	2 0 2			1.6292	1	4 1 4
96	3.021	3.0171	69	2 1 2	4	1.6203	1.6258	1	4 3 2
13	2.935	2.9317	10	3 1 0			1.6120	2	6 1 0
15	2.801	2.7978	12	3 0 2			1.5878	1	6 1 1
		2.7935	2	3 1 1			1.5257	1	4 4 0
13	2.645	2.6426	12	4 0 0	29	1.5227	1.5242	10	3 3 4
10	2.544	2.5433	9	2 2 2			1.5214	8	6 1 2
14	2.473	2.4727	10	3 1 2	3	1.5046	1.5101	3	7 0 0
		2.4335	1	2 1 3			1.5086	1	4 2 4
		2.4250	1	3 2 0			1.4821	1	5 2 3
15	2.297	2.3013	3	0 0 4			1.4734	1	2 0 6
		2.2917	9	4 0 2	6	1.4684	1.4663	1	3 2 5
2	2.242	2.2486	1	1 0 4			1.4645	2	5 1 4
		2.2375	2	4 1 1			1.4476	1	6 2 1
		2.1637	1	2 2 3	8	1.4337	1.4348	1	7 0 2
10	2.147	2.1533	1	1 1 4			1.4322	4	2 1 6
		2.1455	6	3 2 2			1.4270	1	6 1 3
		2.1197	1	3 1 3	3	1.4064	1.4066	3	3 0 6
2	2.0688	2.0622	1	4 1 2	2	1.3862	1.3868	2	4 3 4
7	2.0353	2.0343	6	3 3 0			1.3707	1	2 2 6
9	1.9954	1.9941	6	2 1 4	2	1.3636	1.3635	1	5 2 4
2	1.9511	1.9522	2	4 2 1			1.3593	1	3 1 6
5	1.9239	1.9267	2	3 0 4			1.3534	1	5 4 0
		1.9211	2	5 0 2	2	1.3398	1.3395	2	7 1 2
3	1.8971	1.9026	1	3 2 3			1.3390	1	5 4 1
		1.8985	2	5 1 0	6	1.3241	1.3268	2	4 0 6
11	1.8597	1.8606	7	3 3 2			1.3203	3	6 1 4
		1.8594	1	5 1 1					

specimen material to researchers; he donated his extensive systematic species collection to the RRUFF Project. Perhaps, his greatest contribution was as one of Mindat's most dedicated, proactive and productive managers.

The new mineral and the name have been approved by the International Mineralogical Association (IMA2016-030). The description is based upon one holotype and two cotype specimens that are deposited in the collections of the Natural History Museum of Los Angeles County, 900 Exposition Boulevard, Los Angeles, CA 90007, USA, catalogue numbers 66266 (holotype), 64057 (cotype; also the holotype for magnesiokoritnigite) and 64080 (cotype; also a cotype for torrecillasite).

Occurrence

The new mineral was found at the Torrecillas mine, Salar Grande, Iquique Province, Tarapacá Region, Chile (~20°58'13″S, 70°8'17″W). Torrecillas Hill,

TABLE 3. Data collection and structure refinement details for currierite.

Diffractometer	Rigaku R-Axis Rapid II
X-ray radiation / power	Mo$K\alpha$ ($\lambda = 0.71075$ Å)/50 kV, 40 mA
Temperature	293(2) K
Structural formula	$Na_{3.95}Ca_{2.74}K_{0.08}Mg_{0.83}(Al_{2.13}Fe_{1.87})(AsO_3OH)_{12}\cdot 9H_2O$
Space group	*P*622
Unit-cell dimensions	$a = 12.2057(9)$ Å
	$c = 9.2052(7)$ Å
V	1187.7(2) Å^3
Z	1
Density (for above formula)	3.122 g·cm^{-3}
Absorption coefficient	9.409 mm^{-1}
F(000)	1071.1
Crystal size (μm)	60 × 20 × 20
θ range	3.39 to 24.97°
Index ranges	$-14 \le h \le 14$, $-14 \le k \le 14$, $-8 \le l \le 10$
Refls collected / unique	5906 / 704; $R_{int} = 0.041$
Reflections with $F_o > 4\sigma(F)$	658
Completeness to $\theta = 24.97°$	98.1%
Max. and min. transmission	0.98 and 0.71
Refinement method	Full-matrix least-squares on F^2
Parameters / restraints	81 / 0
Goof	1.104
Final R indices [$F_o > 4\sigma(F)$]	$R_1 = 0.0226$, $wR_2 = 0.0498$
R indices (all data)	$R_1 = 0.0257$, $wR_2 = 0.0510$
Absolute structure parameter	0.026(15)
Largest diff. peak / hole	+0.63 / –0.31 e/A^3

*$R_{int} = \Sigma|F_o^2 - F_o^2(\text{mean})|/\Sigma[F_o^2]$. Goof = $S = \{\Sigma[w(F_o^2 - F_c^2)^2]/(n-p)\}^{1/2}$. $R_1 = \Sigma||F_o| - |F_c||/\Sigma|F_o|$. $wR_2 = \{\Sigma[w(F_o^2 - F_c^2)^2]/\Sigma[w(F_o^2)^2]\}^{1/2}$; $w = 1/[\sigma^2(F_o^2) + (aP)^2 + bP]$ where a is 0.0193, b is 2.2004 and P is $[2F_c^2 + \text{Max}(F_o^2, 0)]/3$.

on which the Torrecillas mine is located, is composed of four different rock units. The Coastal Range Batholith (mainly gabbros) extends from the seashore to the Pan-American Road along the base of Torrecillas Hill. At the foot of Torrecillas Hill is a small area of contact metamorphic rocks in which garnet crystals occur in metamorphosed shales. Higher on the hill, the rocks are predominantly andesites and porphyritic lavas of the Jurassic La Negra Formation. The Torrecillas deposit, in which the new mineral is found, consists of two main veins rich in secondary arsenic and copper minerals that intersect metamorphosed marine shales and lavas. These mineralized veins are genetically related to the aforementioned andesites and porphyritic lavas of the Jurassic La Negra Formation. More information on the geology and mineralogy of the area is provided by Gutiérrez (1975).

The rare secondary chlorides, arsenates and arsenites have been found at three main sites on the hill: an upper pit measuring ~8 m long and 3 m deep, a lower pit ~100 m from the upper pit and measuring ~5 m long and 3 m deep, and a mine shaft adjacent to the lower pit and lower on the hill. Currierite has been found in the upper pit and in the vicinity of the mine shaft.

The new mineral is a secondary alteration phase occurring in association with anhydrite, canutite, chudobaite, halite, lavendulan, magnesiokoritnigite, quartz, scorodite and torrecillasite. The secondary assemblages at the Torrecillas deposit are interpreted as having formed from the oxidation of native arsenic and other As-bearing primary phases, followed by later alteration by saline fluids derived from evaporating meteoric water under hyperarid conditions (*cf.* Cameron *et al.*, 2007).

Physical and optical properties

Currierite occurs as hexagonal prisms, needles and hair-like fibres up to ~200 μm long, in sprays (Fig. 1). Crystals exhibit the forms {100} and

TABLE 4. Atom coordinates and displacement parameters (Å^2) for currierite.

	x/a	*y/b*	*z/c*	U_{eq}	U^{11}	U^{22}	U^{33}	U^{23}	U^{13}	U^{12}
As	0.24262(5)	0.45889(5)	0.24410(6)	0.0186(2)	0.0231(3)	0.0175(3)	0.0144(3)	0.0012(3)	–0.0039(3)	0.0097(2)
Na	1/2	1/2	1/2	0.061(2)	0.098(5)	0.098(5)	0.033(3)	0.000	0.000	0.083(6)
Ca	0	1/2	0	0.0200(10)	0.0200(18)	0.0220(13)	0.0174(15)	0.000	0.000	0.0100(9)
Mg	0	0	0	0.026(4)	0.023(4)	0.023(4)	0.034(6)	0.000	0.000	0.011(2)
Al1	1/3	2/3	1/2	0.0139(10)	0.0176(12)	0.0176(12)	0.0067(14)	0.000	0.000	0.0088(6)
Al2	1/3	2/3	0	0.0136(10)	0.0151(13)	0.0151(13)	0.0106(15)	0.000	0.000	0.0075(6)
O1	0.3396(4)	0.5400(4)	0.3822(4)	0.0179(9)	0.019(2)	0.022(2)	0.0149(19)	–0.0001(18)	–0.0038(17)	0.0110(18)
O2	0.3094(4)	0.3855(4)	0.1570(5)	0.0287(10)	0.044(3)	0.027(2)	0.023(2)	–0.001(2)	–0.004(2)	0.024(2)
O3	0.2032(4)	0.5372(3)	0.1219(4)	0.0158(8)	0.0167(19)	0.018(2)	0.0141(19)	0.0012(17)	0.0000(17)	0.0100(17)
OH4	0.1033(4)	0.3520(5)	0.3223(5)	0.0437(15)	0.027(3)	0.049(3)	0.033(3)	0.022(2)	0.001(2)	0.002(2)
OW5	0	0	0.228(2)	0.155(11)	0.202(17)	0.202(17)	0.061(13)	0.000	0.000	0.101(8)
OW6	0.949(4)	0.130(4)	0.981(8)	0.13(3)	0.29(12)	0.18(6)	0.05(3)	0.03(3)	0.03(4)	0.21(9)
OW7	0	0.145(2)	1/2	0.26(3)	0.36(5)	0.21(3)	0.26(4)	0.04(4)	0.08(7)	0.18(2)

Occupancies: Ca: $Ca_{0.85}Na_{0.15(3)}$; Mg: 0.83(3); Al1: $Al_{0.498}Fe_{0.502(16)}$; Al2: $Al_{0.569}Fe_{0.431(17)}$; OW6: 0.321(19); OW7: $O_{0.58(6)}Na_{0.084}Ca_{0.030}K_{0.014}$

{001} (Fig 2). No twinning was observed. Currierite crystals are transparent with vitreous lustre and white streak. The mineral does not fluoresce in long- or short-wave ultraviolet light. The Mohs hardness is ~2, based on scratch tests. The tenacity is brittle, but elastic in very thin fibres. The fracture is irregular. There is at least one good cleavage parallel to [001]. The density measured by floatation in a mixture of methylene iodide and toluene is 3.08(2) g cm^{-3} and the calculated density is 3.005 g cm^{-3}. Optically, currierite is uniaxial (–), with $\omega = 1.614(1)$ and $\varepsilon = 1.613(1)$ measured in white light. The mineral is nonpleochroic. The mineral is slowly soluble in dilute HCl at room temperature.

Composition

Five quantitative analyses were performed at the University of Utah on a Cameca SX-50 electron microprobe with four wavelength-dispersive spectrometers utilizing *Probe for EPMA* software. Analytical conditions were: 15 kV accelerating voltage, 10 nA beam current and a beam diameter of 10 μm. Currierite exhibited visible damage under the electron beam. Na experienced a time-dependent decrease in intensity under the electron beam, whereas As sustained an increase; both were accounted for by an exponential fit to the intensity vs. time measurements and extrapolation to zero-time intensity.

No other elements were detected by energy dispersive spectroscopy (EDS). Other likely elements were sought by wavelength dispersive spectroscopy, but none were above the detection limits. Raw X-ray intensities were corrected for matrix effects with a $\phi(\rho z)$ algorithm (Pouchou and Pichoir, 1991). The high analytical total is attributed to partial dehydration under vacuum either during carbon coating or in the microprobe chamber. This H_2O loss results in higher concentrations for the remaining constituents than are to be expected for the fully hydrated phase. Because insufficient material was available for a direct determination of H_2O, the amount of water was calculated on the basis of As + Sb = 12 atoms per formula unit (apfu), charge balance and O + Cl = 57 apfu, as determined by the crystal structure analysis (see below). Analytical data are given in Table 1. Note that EDS analyses of numerous crystals on the holotype specimen showed greater variation in composition than is indicated by the electron probe microanalyses (EPMA); this is particularly true of Fe and Al,

TABLE 5. Selected bond distances (Å) for currierite.

As–O1	1.681(4)	Al1–O1(×6)	1.921(4)	Na–O1(×4)	2.490(4)	Hydrogen bonds	
As–O2	1.685(4)			Na–OH4(×4)	3.132(6)	OH4···O2	2.789(7)
As–O3	1.694(4)	Al2–O3(×6)	1.941(4)	<Na–O>	2.811	OW5···OW7(×2)	3.07(2)
As–OH4	1.701(5)					OW6···O2	2.86(6)
<As–O>	1.690	Mg–OW6(×4)	1.99(2)	Ca–O2(×4)	2.491(5)	OW6···O2	2.98(3)
		Mg–OW5(×2)	2.10(2)	Ca–O3(×4)	2.548(4)		
		<Mg–O>	2.027	<Ca–O>	2.520		

which show a negative correlation, and Na and Ca, which also show a negative correlation.

The empirical formula is $(Na_{3.95}Al_{2.96}Ca_{2.74}Mg_{1.28}Fe^{3+}_{0.63}Cu_{0.13}K_{0.08}Co_{0.03})_{\Sigma 11.80}(As^{5+}_{11.68}Sb^{5+}_{0.32})_{\Sigma 12}(O_{56.96}Cl_{0.04})_{\Sigma 57}H_{30.81}$. The simplified structural formula is $Na_4Ca_3MgAl_4(AsO_3OH)_{12}\cdot 9H_2O$, which requires Na_2O 5.67, CaO 7.70, MgO 1.84, Al_2O_3 9.33, As_2O_5 63.10, H_2O 12.36, total 100 wt.%. The Gladstone-Dale compatibility index $1 - (K_P/K_C)$ for the empirical formula is –0.007, in the superior range (Mandarino, 2007).

X-ray crystallography and structure refinement

Both powder and single-crystal X-ray studies were carried out using a Rigaku R-Axis Rapid II curved imaging plate microdiffractometer, with monochromatic Mo$K\alpha$ radiation. For the powder-diffraction study a Gandolfi-like motion on the φ and ω axes was used to randomize the sample and observed *d*-values and intensities were derived by profile fitting using *JADE 2010* software (Materials Data, Inc.). The powder data presented in Table 2 show good agreement with the pattern calculated from the structure determination. Unit-cell parameters refined from the powder data using *JADE 2010* with whole pattern fitting are $a = 12.1997(10)$, $c = 9.2019(7)$ Å and $V = 1186.7(2)$ Å^3.

The Rigaku *CrystalClear* software package was used for processing the structure data, including the application of an empirical multi-scan absorption correction using *ABSCOR* (Higashi, 2001). The structure was solved in space group *P*622 using

TABLE 6. Bond-valence analysis for currierite. Values are expressed in valence units.

	As	Al1	Al2	Na	Ca	Mg	H4	H5a	H5b	H6a	H6b	Σ
O1	1.26	0.54 ×6↓		0.16 ×4↓								1.96
O2	1.25				0.24 ×4↓		0.19			0.17	0.13	1.98
O3	1.22		0.53 ×6↓		0.21 ×4↓							1.96
OH4	1.20			0.03 ×4↓			0.81					2.04
OW5						0.33 ×2↓		0.88	0.88			2.09
OW6						0.45 ×4↓				0.83	0.87	2.15
Σ	4.93	3.24	3.18	0.76	1.80	2.46	1.00	1.00*	1.00*	1.00	1.00	

* The partially occupied OW7 site is not included in the bond-valence analysis, although the hydrogen bond contributions from OW5 to OW7 (0.12 valence units) are accounted for. Multiplicities are indicated by ×↓. Bond strengths for the Al1 and Al2 sites are based on the refined occupancies; other sites are based on full occupancies by their ideal occupants. The Na^+–O bond-valence parameters are from Wood and Palenik (1999); As^{5+}–O, Al^{3+}–O, Fe^{3+}–O, Ca^{2+}–O and Mg^{2+}–O from Brown and Altermatt (1985); hydrogen-bond strengths based on O···O bond lengths also from Brown and Altermatt (1985).

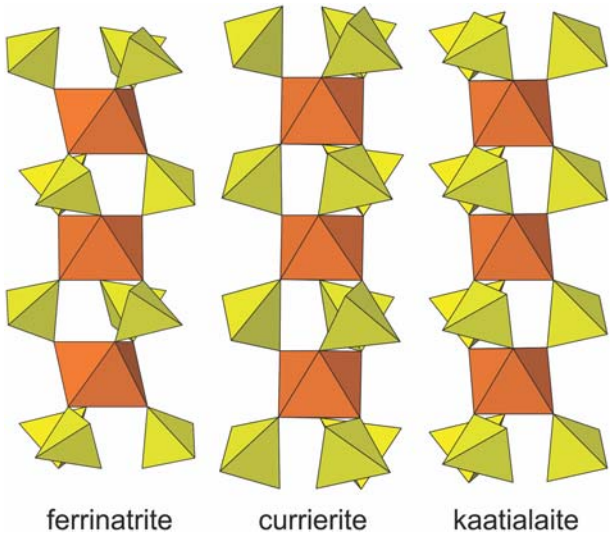

FIG. 3. The chains of octahedra and tetrahedra in ferrinatrite, currierite and kaatialaite. Note that the chain in currierite is a mirror image of that in kaatialaite, but that is related to merohedral twinning in currierite. This chain is a geometrical isomer of that in ferrinatrite.

SIR2011 (Burla *et al.*, 2012). *SHELXL-2013* (Sheldrick, 2015) was used for the refinement of the structure. Structure solutions were attempted in all 16 hexagonal and trigonal space groups with no systematic extinctions, but only *P*622 provided a good solution and refinement. The location of most atom sites was straightforward.

The octahedrally coordinated sites in the chain were identified initially as Al, but were subsequently refined as being jointly occupied by Al and Fe although the sites could presumably also accommodate minor Cu, Co and/or Mg. The Na and Ca sites between the chains were assigned based upon scattering power and bond valence. The Na site refined to full occupancy by Na, although its displacement parameters were notably high. The Ca site was subsequently refined with joint occupancy by Ca and Na. The Mg site on a 6-fold axis was assigned based upon scattering power and surrounding bond lengths. The OW5 site, also on this axis, accounts for two apical O atoms of an MgO_6 octahedron; an approximately 1/3 occupied 12-fold OW6 site accounts for the four disordered O atoms around the girdle of this octahedron. Notably, the Mg–OW6 distance is too short, which results in a very high Mg bond-valence sum of 2.46 valence units. The OW6 site has very high displacement parameters, so the short Mg–OW6 distance may be an artefact of the refinement; however, attempts to refine the structure in lower symmetry space groups, including *P*1, provided similar O site placements (and much higher *R* factors). On the other hand, the refinement in *P*1 provided full occupancy for the Mg site, suggesting that the low refined Mg occupancy in *P*622 (0.83) may be an artefact. An additional partially occupied site (OW7) apparently corresponds to an isolated H_2O group, but could also accommodate large cations (Na, Ca and/or K) and perhaps even medium-sized cations.

The Na and Ca sites together provide 3.45 Na and 2.55 Ca apfu, significantly lower than the amounts found by EPMA (3.95 Na and 2.74 Ca). The OW7 site has a scattering power of 38.4 e^-. The deficiencies in Na and Ca (and the 0.08 K in the empirical formula) could be rectified by assigning the OW7 site an occupancy of 8.4% Na, 3.0% Ca, 0.7% K and 58.3% O. In the final refinement, the OW7 site was assigned this joint occupancy. The occupancy of the Al sites indicated by the structure refinement is considerably higher in Fe *vs.* Al than in the empirical formula. Although some Cu and Co content would elevate the apparent Fe, we attribute this difference mostly to a real Fe *vs.* Al compositional difference between the crystal used for the structure refinement and those analysed by EPMA. As noted above, EDS analyses of numerous crystals on the holotype specimen indicate that the structure crystal could vary significantly from the crystals analysed by EPMA in Na:Ca and Fe:Al, as well as in contents of other cations.

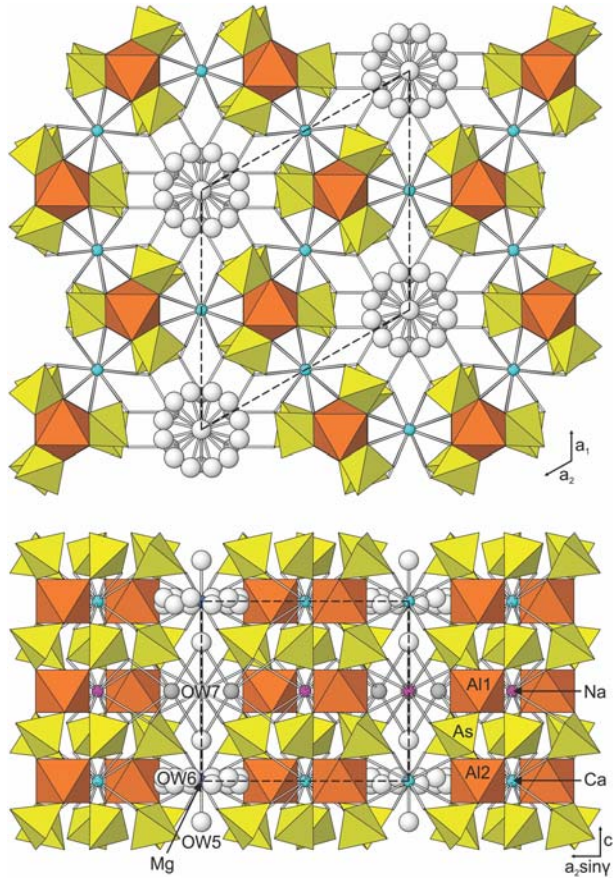

FIG. 4. The crystal structure of currierite viewed along **c** (top) and along $\mathbf{a_1}$ (bottom). The unit cell outlines are shown by dashed black lines.

Data collection and refinement details are given in Table 3, atom coordinates and displacement parameters in Table 4, selected bond distances in Table 5 and a bond-valence analysis in Table 6.

Discussion

The structure of currierite is based upon a heteropolyhedral chain along **c** in which AlO_6 octahedra are triple-linked by sharing corners with AsO_3OH tetrahedra (Fig. 3) such that all of the vertices of octahedra link to tetrahedra and half of the vertices of tetrahedra link to octahedra. Chains are linked to one another by bonds to 8(4 + 4)-coordinated Na and 8-coordinated Ca forming a three-dimensional framework with large cavities (Fig. 4). The cavities contain rotationally disordered $Mg(H_2O)_6$ octahedra, which only link to the framework via hydrogen bonds. Another partially occupied site in the cavity can probably accommodate either Na or H_2O.

The chain in the structure of currierite is identical to that in kaatialaite (Boudjada and Guitel, 1981), $Fe[AsO_2(OH)_2]\cdot 5H_2O$, except that in currierite only one unshared arsenate corner is an OH group, while in kaatialaite both unshared arsenate corners are OH groups. Note that these chains as depicted in Fig. 3 are mirror images of one another, but this is related to the merohedral twinning in the currierite structure. These chains are topologically the same as that in the structure of ferrinatrite (Scordari, 1977), $Na_3(H_2O)_3[Fe(SO_4)_3]$, although the ferrinatrite chain is a geometrical isomer of those in currierite and kaatialaite (Fig. 3).

The chains in the structure of kaatialaite are only linked via hydrogen bonds to isolated H_2O groups

between the chains. Ferrinatrite has greater structure similarity to currierite in that the chains in the ferrinatrite structure are linked via bonds to Na atoms between the chains thereby yielding a three-dimensional framework; however, beyond that, the structures are quite distinct.

Acknowledgements

Editorial Board Member Andrew Christy, Structures Editor Peter Leverett and reviewer Francesco Demartin are thanked for their constructive comments on the manuscript. A portion of this study was funded by the John Jago Trelawney Endowment to the Mineral Sciences Department of the Natural History Museum of Los Angeles County.

References

Boudjada, A. and Guitel, J.C. (1981) Structure cristalline d'un orthoarsénate acide de fer(III) pentahydraté: Fe $(H_2AsO_4)_3 \cdot 5H_2O$. *Acta Crystallographica*, **B37**, 1402–1405.

Brown, I.D. and Altermatt, D. (1985) Bond–valence parameters from a systematic analysis of the inorganic crystal structure database. *Acta Crystallographica*, **B41**, 244–247.

Burla, M.C., Caliandro, R., Camalli, M., Carrozzini, B., Cascarano, G.L., Giacovazzo, C., Mallamo, M., Mazzone, A., Polidori, G. and Spagna, R. (2012) *SIR2011*: a new package for crystal structure determination and refinement. *Journal of Applied Crystallography*, **45**, 357–361.

Cameron, E.M., Leybourne, M.I. and Palacios, C. (2007) Atacamite in the oxide zone of copper deposits in northern Chile: involvement of deep formation waters? *Mineralium Deposita*, **42**, 205–218.

Currier, R.H. (1995) The Bolivian death switch. *Mineralogical Record*, **26**, 195–200.

Currier, R.H. (2008*a*) About mineral collecting – part 1. *Mineralogical Record*, **39**, 305–313.

Currier, R.H. (2008*b*) About mineral collecting – part 2. *Mineralogical Record*, **39**, 409–418.

Currier, R.H. (2009*a*) About mineral collecting – part 3. *Mineralogical Record*, **40**, 49–59.

Currier, R.H. (2009*b*) About mineral collecting – part 4. *Mineralogical Record*, **40**, 165–176.

Currier, R.H. (2009*c*) About mineral collecting – part 5. *Mineralogical Record*, **40**, 194–202.

Gutiérrez, H. (1975) *Informe sobre una rápida visita a la mina de arsénico nativo, Torrecillas*. Instituto de Investigaciones Geológicas, Iquique, Chile.

Higashi, T. (2001) *ABSCOR*. Rigaku Corporation, Tokyo.

Kampf, A.R., Sciberras, M.J., Williams, P.A., Dini, M. and Molina Donoso, A.A. (2013*a*) Leverettite from the Torrecillas mine, Iquique Provence, Chile: the Co–analogue of herbertsmithite. *Mineralogical Magazine*, **77**, 3047–3054.

Kampf, A.R., Nash, B.P., Dini, M. and Molina Donoso, A.A. (2013*b*) Magnesiokoritnigite, $Mg(AsO_3OH) \cdot H_2O$, from the Torrecillas mine, Iquique Province, Chile: the Mg–analogue of koritnigite. *Mineralogical Magazine*, **77**, 3081–3092.

Kampf, A.R., Mills, S.J., Hatert, F., Nash, B.P., Dini, M. and Molina Donoso, A.A. (2014*a*) Canutite, $NaMn_3[AsO_4]_2[AsO_2(OH)_2]$, a new protonated alluaudite–group mineral from the Torrecillas mine, Iquique Province, Chile. *Mineralogical Magazine*, **78**, 787–795.

Kampf, A.R., Nash, B.P., Dini, M. and Molina Donoso, A.A. (2014*b*) Torrecillasite, $Na(As,Sb)_4^{3+}O_6Cl$, a new mineral from the Torrecillas mine, Iquique Province, Chile: description and crystal structure. *Mineralogical Magazine*, **78**, 747–755.

Kampf, A.R., Nash, B.P., Dini, M. and Molina Donoso, A.A. (2016*a*) Chongite, $Ca_3Mg_2(AsO_4)_2(AsO_3OH)_2 \cdot 4H_2O$, a new arsenate member of the hureaulite group from the Torrecillas mine, Iquique Province, Chile. *Mineralogical Magazine*, **80**, 1255–1263.

Kampf, A.R., Nash, B.P., Dini, M. and Molina Donoso, A.A. (2016*b*) Gajardoite, $KCa_{0.5}As_4^{3+}O_6Cl_2 \cdot 5H_2O$, a new mineral related to lucabindiite and torrecillasite from the Torrecillas mine, Iquique Province, Chile. *Mineralogical Magazine*, **80**, 1265–1272.

Kampf, A.R., Nash, B.P., Dini, M., Molina Donoso, A.A. (2016*c*) Juansilvaite, $Na_5Al_3[AsO_3(OH)]_4[AsO_2(OH)_2]_2(SO_4)_2 \cdot 4H_2O$, a new arsenate-sulfate from the Torrecillas mine, Iquique Province, Chile. *Mineralogical Magazine*, **80**, 619–628.

Mandarino, J.A. (2007) The Gladstone–Dale compatibility of minerals and its use in selecting mineral species for further study. *The Canadian Mineralogist*, **45**, 1307–1324.

Pouchou, J.-L. and Pichoir, F. (1991) Quantitative analysis of homogeneous or stratified microvolumes applying the model "PAP." Pp. 3l–75 in: *Electron Probe Quantitation* (K.F.J. Heinrich and D.E. Newbury, editors). Plenum Press, New York.

Scordari, F. (1977) The crystal structure of ferrinatrite, $Na_3(H_2O)_3[Fe(SO_4)_3]$ and its relationship to Maus's salt, $(H_3O)_2K_2\{K_{0.5}(H_2O)_{0.5}\}_6[Fe_3O(H_2O)_3(SO_4)_6](OH)_2$. *Mineralogical Magazine*, **41**, 375–383.

Sheldrick, G.M. (2015) Crystal structure refinement with SHELXL. *Acta Crystallographica*, **C71**, 3–8.

Wood, R.M. and Palenik, G.J. (1999) Bond valence sums in coordination chemistry. Sodium-oxygen complexes. *Inorganic Chemistry*, **38**, 3926–3930.